Materials Characterization 196 (2023) 112636

Contents lists available at ScienceDirect

Materials Characterization

journal homepage: www.elsevier.com/locate/matchar

What are the Tower's method products: Metal-hydroxides or metal-glycerolates?

Josué M. Gonçalves [a,b,*,1], Irlan S. Lima [b,1], Abhijit H. Phakatkar [c], Rafael S. Pereira [d], Paulo R. Martins [e], Koiti Araki [b], Lúcio Angnes [b,**], Reza Shahbazian-Yassar [a,*]

[a] Department of Mechanical and Industrial Engineering, University of Illinois at Chicago, Chicago, IL 60607, United States
[b] Instituto de Química, Universidade de São Paulo, Av. Prof. Lineu Prestes 748, 05508-000 São Paulo, SP, Brazil
[c] Department of Biomedical Engineering, University of Illinois at Chicago, Chicago, IL 60607, USA
[d] Centro de Engenharia, Modelagem e Ciências Sociais Aplicadas, Universidade Federal do ABC, 09210-580 Santo André, SP, Brazil
[e] Instituto de Química, Universidade Federal de Goiás, Av. Esperança s/n, 74690-900 Goiânia, GO, Brazil

ARTICLE INFO

Keywords:
Synthesis
Tower's method
Nickel hydroxide
Nickel-glycerolate
Transmission electron microscopy

ABSTRACT

It has been long believed that colloidal nickel hydroxide nanoparticles are produced by the reaction of nickel salts, glycerol and potassium hydroxide known as the Tower method. In the present work, we challenge this belief and reveal the reasons for error in identification of nickel products produced by the Tower method. We propose that Ni-based precursor complexes are the primary products of the Tower method reaction, and these precursors undergo transition to layered Ni-glycerolate derivatives upon thermal treatment. We demonstrated the presence of Ni^{2+} coordinated to different types of O-donor ligands (glycerol, glycerolate ion, acetate ion and/or OH^-) forming Ni-complex precursors. Using *in-situ* transmission electron microscopy, we showed that Ni-based precursor complexes can be converted to nickel nanoparticles upon exposure to electron beam, but no evidence of nickel hydroxide nanoparticle formation was found. The nickel hydroxide nanoparticles are only formed upon further reaction of Ni-glycerolate precursors with an aqueous alkaline solution. Those new findings shed light on the nature of the metal derivatives obtained by the reaction of Ni^{2+} and glycerol in the Tower method and provide more solid foundation to design electrode materials for batteries, supercapacitors, electrocatalysts and electrochemical sensors.

1. Introduction

The method of synthesis of colloidal nickel hydroxide proposed by Tower almost a century ago [1] was adapted over time and has been widely used more recently [2]. Nonetheless, the X-ray diffraction pattern of the generated "nickel-hydroxide" is analogous to other layered materials with similar chemical composition, especially of Ni-glycerolates prepared by solvothermal process (Fig. 1). In fact, the crystal structure of the material actually produced in the reaction of nickel salts and glycerol (in the presence or absence of potassium hydroxide) is not clearly defined yet, despite been extensively used in the preparation of nanomaterials for electrochemical applications, adding to the uncertainties regarding the nature of that material and its crystal structure. For instance, many mono- and bimetallic transition metal hydroxides have been prepared using such a strategy, especially based on the sol-gel method reported by Tower [1] and by Rocha and collaborators [2]. Basically, the synthesis reported by Rocha et al. [2] consists of dissolving the metal-acetate in glycerin at 50 °C, under vigorous stirring, cooling down to room temperature and then reacting with 1:2 M ratio of KOH in *n*-butanol (Fig. 1a), and keeping the reaction mixture under stirring for six hours. Interestingly, the electroactive materials prepared in this way and subjected to thermal treatment at 240 °C for 30 min in an oven exhibit enhanced stability for repeated redox cycling, indicating that thermal treatment plays a key role in defining the electrode material properties [2] for energy storage application.

Nickel hydroxide ($Ni(OH)_2$) derivatives are known to be versatile and multifunctional materials, that are being explored as

* Corresponding authors at: Department of Mechanical and Industrial Engineering, University of Illinois at Chicago, Chicago, IL 60607, United States.
** Corresponding author.
E-mail addresses: jmart437@uic.edu (J.M. Gonçalves), luangnes@iq.usp.br (L. Angnes), rsyassar@uic.edu (R. Shahbazian-Yassar).
[1] Equal contributors.

https://doi.org/10.1016/j.matchar.2022.112636
Received 19 November 2022; Received in revised form 27 December 2022; Accepted 28 December 2022
Available online 30 December 2022

electrocatalysts for water-splitting [3] and electrochemical sensors [4], and as active materials in electrochromic devices [5], nickel–metal hydride (NiMH) batteries [6], hybrid supercapacitors [7] and light-stimulated actuators [8]. Many mono- and bimetallic Ni-based hydroxides prepared by Tower's method were recently reported and all presented a diffraction peak at around 10.6°, assigned to the (003) reflection, as expected for layered alpha-nickel hydroxide phase materials (α-$Ni(OH)_2$) [9–11]. For instance, Gomes et al. [9] described that α-$Ni(OH)_2$ nanoparticles with 25% of Mn^{2+} (named α-NiMn-hydroxide) exhibited outstanding electrochemical and charge–discharge properties, evidenced by the high specific charge capacity of 417.5C g^{-1}, more than three times larger than for α-$Ni(OH)_2$, allied to an excellent charge retention capacity of 86.5%, even after 5000 galvanostatic charge–discharge processes at 25 A g^{-1}. Curiously, metal-glycerolates (M-Gly), another class of layered materials that have been extensively reported in recent years [12], also show a diffraction peak at 10.6°. For example, a facile solvothermal method was described by Ding et al. [13] to synthesize micron-sized NiMn-glycerolate (NiMn-Gly) solid spheres exhibiting a diffraction peak at 10.68°, corresponding to the interlayer spacing of a lamellar material exhibiting a structure made of stacked metal−oxygen sheets separated by glycerolate anions [14]. The question is "what nickel material has been obtained by Tower's method: the hydroxide ($Ni(OH)_2$) or the glycerolate?

It is easy to notice the structural similarity of NiMn-Gly and aforementioned α-NiMn-hydroxide nanoparticles after heat processing at 240 °C, despite the apparent differences. The first one is supposed to be stacked nickel and manganese hydroxide layers with counterions and other molecules in the interlamellar space, whereas the last one has a structure of nickel and manganese cations bridged by glycerolate ligands generating a material that is better described as a coordination polymer. In this case, the coordination of glycerolate ions to the metal ions (Ni and Mn) leading to formation of M-Gly microspheres is induced by the solvothermal processing at 180 °C, for 10 h (Fig. 2b). Similarly, the enhanced electrochemical stability of NiMn-hydroxide is achieved upon thermal processing at 240 °C where water is evaporated out favoring the deprotonation processes generating glycerolate ligands. In addition, the electrode modified with NiMn-Gly microspheres delivered a specific capacitance of 719C g^{-1} at the current density of 1.0 A g^{-1}, a charge-capacity superior to that of α-$Ni(OH)_2$.

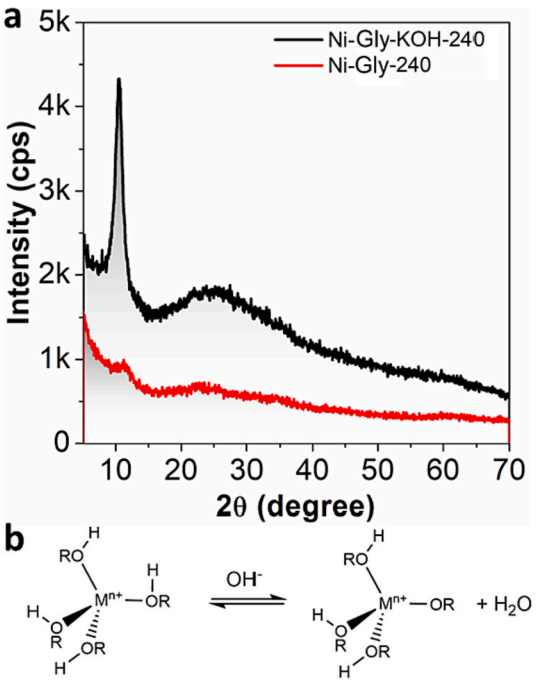

Fig. 2. (a) XRD pattern of Ni-Gly-KOH-240 (black line) and Ni-Gly-240 (red line). (b) More or less organized metal hydroxide/acetate lamellar material should be formed upon addition of KOH and heat treatment, but only acetate can act as bridging ligand connecting the metal ions thus generating ordered materials in a much shorter range. (For interpretation of the references to colour in this figure legend, the reader is referred to the web version of this article.)

It is also important to highlight that most of the works describing the development of materials prepared by the Tower's method, or other similar reactions, describe the characterization of the $Ni(OH)_2$ nanoparticles (colloidal solution of nickel hydroxide) after a dialysis or "washing" process to eliminate the excess of glycerol [2]. However, there is a great possibility of Ni-Gly been the actual product of the

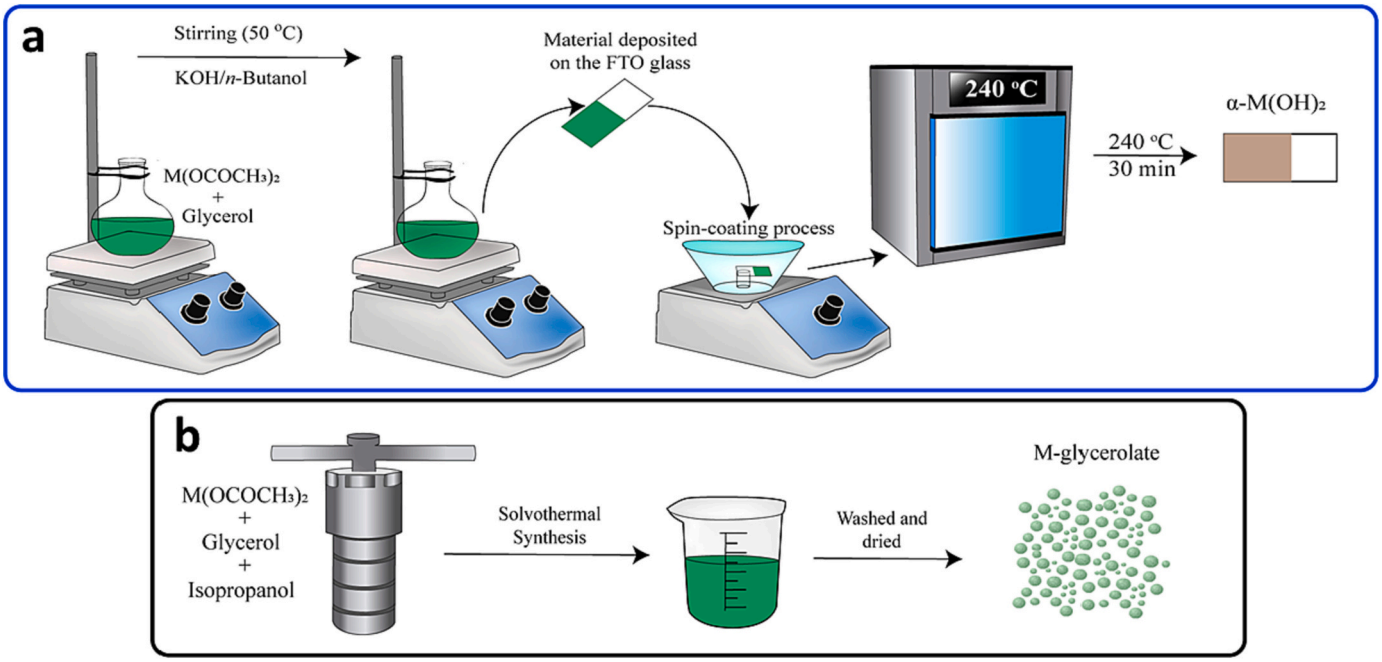

Fig. 1. (a) Scheme showing the sol-gel synthesis adapted from Tower's method; and (b) Conventional solvothermal synthesis of M-glycerolate.

Tower's method, where the metal hydroxides are generated only after the heat treatment. In fact, Khonina et al. [15] reported that the reactions of iron(II) or iron(III) cations with glycerol proved to proceed only in the presence of an equivalent amount of sodium hydroxide to give glycerolates with various chemical compositions, as confirmed by Mössbauer and infrared spectroscopy, X-ray diffractometry and elemental analysis. Accordingly, $Ni(OH)_2$ nanoparticles may be formed during the dialysis or "washing" step of the material, since water can promote the hydrolysis of Ni-Gly [16,17].

Hereon we report a systematic characterization of Ni and/or NiCo-based electrode materials prepared by Tower's method, comparing the products generated in the presence and absence of KOH to elucidate their structures. In particular, unveiled are the structural properties of the resultant materials before the thermal processing at 240 °C and the dialysis or "washing" step, and after these processes, as well as their electrochemical properties, in order to shed light on that fundamental question.

2. Experimental

All reagents and solvents were of analytical grade and used as received. Anhydrous glycerin, isopropyl alcohol, *n*-butyl alcohol and potassium hydroxide (KOH) were purchased from Synth. Nickel acetate tetrahydrate ($Ni(CH_3COO)_2{\cdot}4H_2O$) was obtained from Sigma-Aldrich, whereas cobalt acetate tetrahydrate ($Co(CH_3COO)_2{\cdot}4H_2O$) was acquired from Synth. All aqueous solutions were prepared with ultrapure deionized water from a MilliQ purification system (DI-water, $\rho \geq 18.2$ MΩ cm).

2.1. Preparation of Ni-Gly-KOH and Ni-Gly

The Ni-Gly-KOH was prepared as previously reported [18], by dissolving 4.82 mmol of nickel acetate tetrahydrate ($Ni(CH_3COO)_2{\cdot}4H_2O$) in 25 mL of anhydrous glycerin at 50 °C. Then, 9.64 mmol of KOH, dissolved in 25 mL of anhydrous *n*-butanol, was added dropwise into the stirred solution of nickel acetate, at room temperature. Ni-Gly corresponds simply to the previously prepared nickel acetate solution in anhydrous glycerin. The bimetallic nickel–cobalt materials (Ni_xCo_{1-x}-Gly), where x = 0.6, was prepared similarly to pure nickel derivatives, in the presence and absence of KOH, as ascribed above, and denoted as NiCo-Gly-KOH and NiCo-Gly, respectively.

The Ni-Gly-KOH-180 and Ni-Gly-KOH-240, and the Ni-Gly-180 and Ni-Gly-240 samples were prepared as films by depositing the respective non-thermally treated materials on glass slips and vacuum drying them at 180 or 240 °C for 30 min. The materials were carefully characterized by spectroscopic, XRD and electron microscopy techniques to determine their morphology and structure.

2.2. Preparation of Ni-Gly-KOH-240 and Ni-Gly-240 modified FTO electrodes

Fluorine doped tin oxide (FTO) glass pieces (1.0 × 2.5 cm) were carefully washed with soap and rinsed with isopropanol:water (1:1) mixture. Then, a 1 cm^2 area was delimited on the surface with a scotch tape and 100 μL of Ni-Gly-KOH, or Ni-Gly, was spin-coated on them. In sequence, the tape was removed, and the modified electrode heated at 240 °C for 30 min to produce stable films of the monometallic materials. The same procedure was adopted for the bimetallic materials NiCo-Gly-KOH-240 and NiCo-Gly-240.

2.3. Characterization

The samples were characterized by X-ray diffractometry (XRD) in a Bruker D2 Phaser diffractometer equipped with a Cu Kα source (λ = 1.5418 Å, 30 kV, 15 mA, step = 0.05°), in the 2theta range from 5 to 70°. Infrared spectra were recorded in a Bruker ALPHA Fourier-transform infrared spectroscopy (FTIR) spectrophotometer. UV–vis absorption spectra were registered in a Hewlett Packard 8453A diode-array UV–Vis spectrophotometer, in the 190 to 1100 nm range, using 10.0 mm quartz cuvettes.

Chemical surface analyses were carried out by X-ray photoelectron spectroscopy (XPS), using a K-Alpha X-ray photoelectron spectrometer (Thermo Fisher Scientific, UK), equipped with a hemispherical electron analyzer and an Al Kα microfocused monochromatized source with resolution of 0.1 eV. Survey (full-range) and high-resolution spectra for carbon were acquired using a spot size of 400 μm and pass energy of 200 and 50 eV, respectively. The data were analyzed using the Thermo Avantage Software (Version 5.921).

Transmission electron microscopy (TEM) and high-resolution transmission electron microscopy (HRTEM) images were collected by a JEOL ARM200CF equipment. Energy dispersive X-ray spectroscopy (EDS) was performed using an aberration corrected JEOL ARM200CF equipment with a cold field emission gun operated at 200 kV, and equipped with an Oxford X-max 100TLE windowless X-ray detector.

Cyclic voltammetry measurements were carried out using an Eco-Chemie Autolab PGSTAT30 potentiostat/galvanostat and a conventional three electrodes cell, constituted by the modified FTO working electrode, an Ag/AgCl (3.0 mol L^{-1} in KCl) reference, and a platinum wire as the counter electrode.

3. Results and discussion

Tower's method, and other similar protocols, have been widely reported in the literature aiming the preparation of electroactive materials based on $Ni(OH)_2$ for different applications, especially electrode materials for batteries and supercapacitors, electrocatalysts and electrochemical sensors. This multifunctionality is mainly associated with the presence of $Ni^{2+/3+}$ ions that act as active sites, but organic compounds are present in considerable amounts even after exhaustive attempts of purification by washing, dialysis, and/or thermal treatment at 240 °C for 30 min [19–21]. Furthermore, the unexpected similarity of the Ni-Gly and α-$Ni(OH)_2$ XRD patterns clearly indicates that more studies are fundamental to unravel the actual structure of the generated materials, especially in the Tower's method and in other similar reactions using glycerol as solvent.

In that regard, Ni-Gly-KOH-240 (and NiCo-Gly-KOH-240), prepared as described by Rocha et al. [2], was compared with the material prepared by thermal processing in the absence of KOH (Ni-Gly-240). Initially the material precursors were characterized by XRD. Interestingly, KOH seems to increase the degree of crystallinity of the material generated after thermal treatment at 240 °C for 30 min (named Ni-Gly-KOH-240), as confirmed by the rise of a sharp peak around 10.5° almost absent in the Ni-Gly-240 material obtained in the same conditions, except for the KOH (Fig. 2a). Similar result was obtained for the bimetallic NiCo system (NiCo-Gly-KOH-240 and NiCo-Gly-240), as shown in Fig. S1.

The presence of the diffraction peak at 10.5° does not provides conclusive information about what is formed upon heat treatment since it is in the 2θ range that can be attributed to both α-$Ni(OH)_2$ and Ni-Gly, as reported in the literature and listed in Table S1. The appearance of an intense diffraction peak at 10.5° in the XRD of Ni-Gly-KOH-240 must be related to the formation of more or less organized lamellar structures due to the presence of hydroxyl bridging ligands connecting the Ni^{2+} ions, as well as acetate ligands, and/or glycerolate ligands formed by reaction of glycerol with hydroxide, and elimination of water during the thermal treatment process. In the absence of KOH this reaction is improbable and only acetate can act as a weaker bridging ligand, as schematized in Fig. 2b, leading to the formation of structures with much shorter range of organization (small peak at ~11°). In fact, in the absence of KOH, the formation of alcoholate metal complexes such as with glycerolate (pKa = 14.4) is not sufficiently favored, but the equilibrium can be significantly shifted by OH^- (pKa ~ 14) given its similar

basicity.

In fact, the Tower's method is basically about the preparation of nickel hydroxide nanoparticles gels that can be more or less easily peptidized, as discussed in the literature [1]. The Ni^{2+} and KOH stoichiometry was changed to 1:2 in the modified method to consistently get clear "sols", as described by Rocha et al. [2]. Nevertheless, the characteristic electrochemical features of "$Ni(OH)_2$ in the alpha phase (α-$Ni(OH)_2$)" only become apparent upon heat treatment at 240 °C for 30 min, demonstrating the key role of this process. In addition, clearly demonstrate the possibility that the actual material generated in the process may not be the one expected. To shed light on this question, a detailed transmission electron microscopy study was carried out analyzing the Ni-Gly-KOH by *in-situ* TEM. Thereunto, an aliquot of Ni-Gly-KOH sol (Fig. S2), prepared by the modified Tower's method, was diluted in isopropanol, deposited on a copper grid covered with amorphous lacey carbon film and dried under a heating lamp, at temperatures below 40 °C, to assure the integrity of the sample.

Interestingly, no nanoparticles could be found in the sol sample after evaporation of isopropanol and n-butanol (Fig. S3 and Fig. 3). This new finding is evidenced by the homogeneous elemental distribution of C, O, K and Ni in the individual EDS mapping, and the composite image of all of them overlayed on the respective STEM image (Fig. S3), showing no evidence of nanoparticles at all. Accordingly, the nanoparticles visualized in the HRTEM images reported by Rocha et al. [2] may be generated in the heating process, or induced *in-situ* by the electron beam during the TEM analysis, as consequence of structural reorganization, nucleation and growth. In fact, the electron beam impinging on the material induced the formation of Ni nanoparticles as shown in Fig. 3. A careful analyses indicated que formation especially of nickel metal nanoparticles, as confirmed by the presence of 0.193 nm apart interference fringes that can be attributed to the (111) planes of cubic phase Ni^0 (Fig. 4a-4b). Similar result is obtained by calcination of the material around 600 °C, as confirmed by the strong magnetism characteristic of nickel metal, demonstrating that glycerol is a good reducing agent at high temperatures and can be useful in the synthesis of Ni^0 nanoparticles [22,23]. In addition, the nanoparticles size showed to be dependent on the thickness of the film exposed to the electron beam (Fig. 4c-4d), as well as the exposure time during the *in-situ* reaction. Using the electron beam to probe the structure and morphology of materials, as well as source of heat and electrons, is very convenient since allow monitoring the evolution of a material as a function of exposition time in detail, providing invaluable information about the evolution process. After a careful study, it was possible to conclude that such a nucleation and growth process does not occur exclusively by mass diffusion type mechanism but involves also the coalescence of nanoparticles (Video 1), especially when the distances between them are lower than 2–3 nm and their size <15 nm [24].

Based on the aforementioned considerations and the XRD/TEM results it is possible to infer that the reaction of $Ni(CH_3COO)_2{\cdot}4H_2O$ in glycerol and in the presence of KOH probably yields solutions containing Ni-glycerolate complexes and/or clusters (Eq. 1). In fact, the formation of metal-glycerolate in the presence and absence of base has been reported in the literature [25]. In addition, no significant differences are observed in the electronic spectra of the materials in the presence and absence of KOH (Fig. 5), indicating that the first coordination sphere in both cases is similar. The presence of the $^3A_{2g}(F) \rightarrow {}^3T_{1g}(P)$ transition around 400 nm, $^3A_{2g}(F) \rightarrow {}^3T_{1g}(F)$ at 670 nm and $^3A_{2g}(F) \rightarrow {}^3T_{2g}(F)$ at 1100 nm suggests the Ni^{2+} ions are coordinated to O-donors [26]. In other words, they are coordinated by acetate, hydroxide and glycerol/glycerolate eventually forming clusters with a bright green clear colour, as expected for Ni^{2+} ions coordinated to those O-donor ligands. In addition, the presence of $Ni(OH)_2$ nanoparticles can be ruled out, as

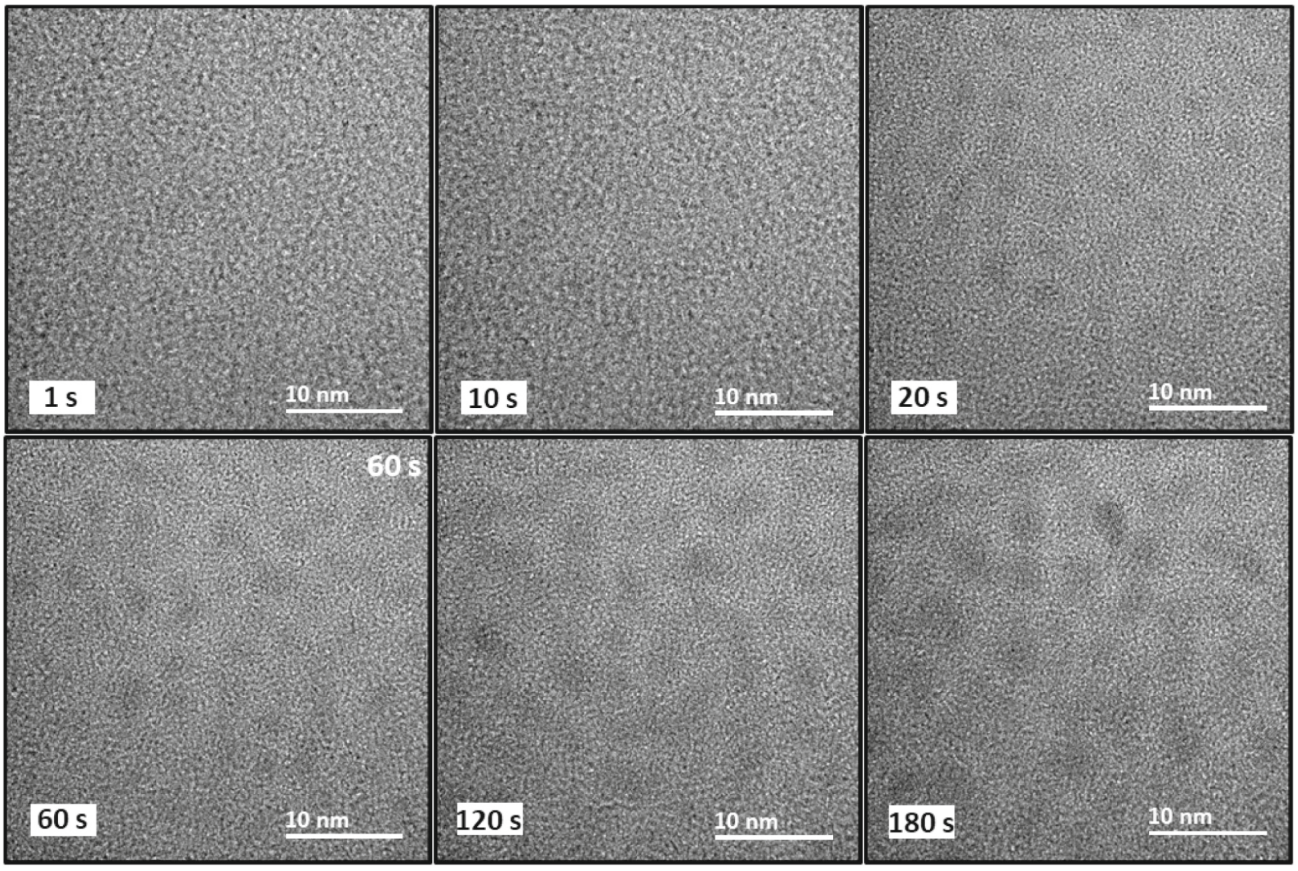

Fig. 3. A series of TEM images of a Ni-Gly-KOH film taken at different e-beam exposure times, monitoring the *in-situ* nucleation and growth of nanoparticles induced by the electron beam.

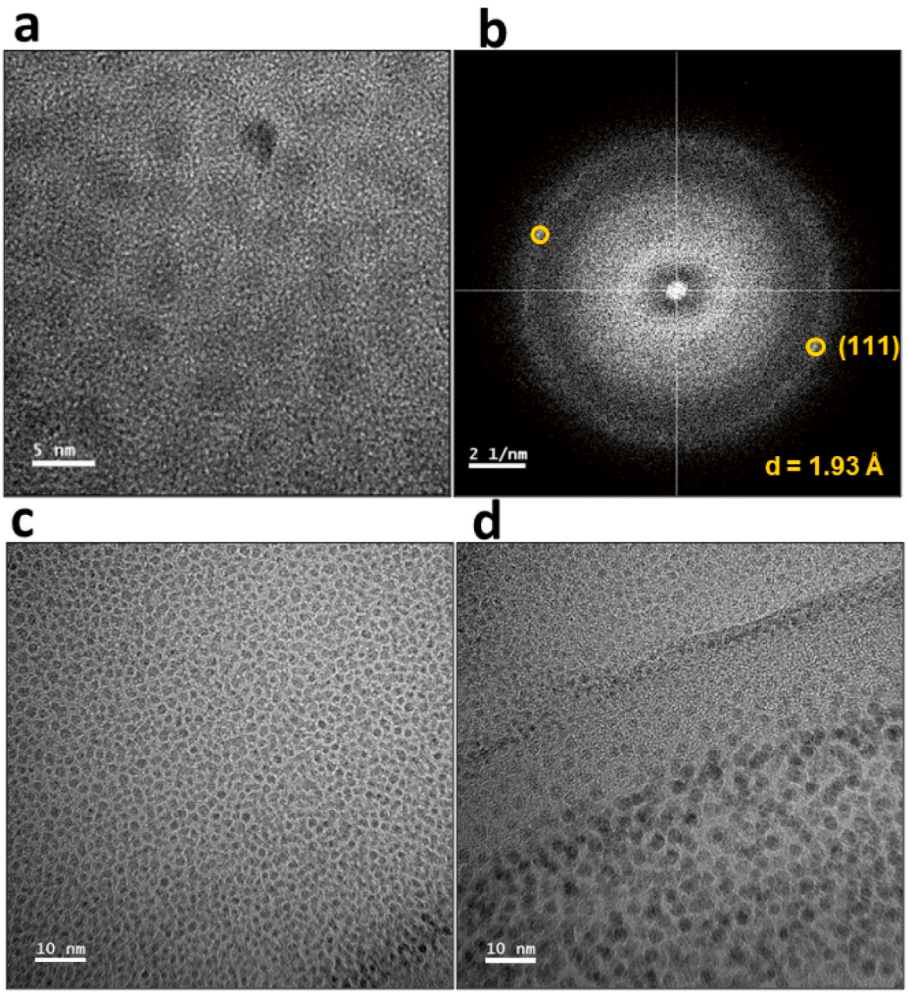

Fig. 4. (a) TEM image and (b) a corresponding fast Fourier transform (FFT) pattern indicating the selected plane corresponding to the Ni cubic crystal structure. (c) Nucleation and growth of Ni nanoparticles induced by the TEM electron beam on lacey carbon support Ni-Gly-KOH film. (d) The amount of precursor influences the growth of Ni nanoparticles induced by the TEM electron beam. The bottom part of the image corresponds to the hole in the lacey carbon support film where a larger amount of precursor material was trapped.

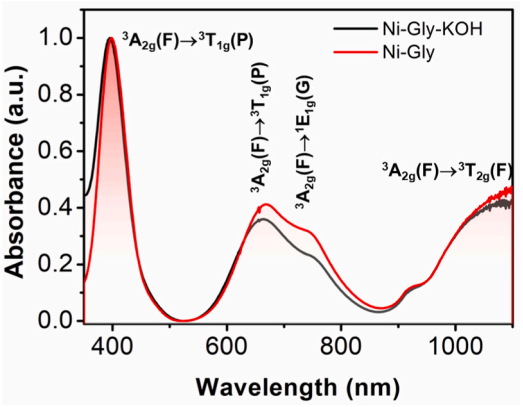

Fig. 5. UV–Vis spectra of Ni-Gly-KOH (black line) and Ni-Gly (red line). (For interpretation of the references to colour in this figure legend, the reader is referred to the web version of this article.)

expected for the insignificant contribution of light scattering in the absorption spectra shown in Fig. 5, and almost not perceptible turbidity (light scattering, Fig. S2). In fact, scattering can greatly modify the UV–Vis spectrum depending on size of the scatterers which can be very different from true absorption and named "extinction spectrum" [27].

$$Ni^{2+} + nL = [Ni(L)n]^{2-} \ (L = 2\,(OH^- + (C_3H_5O_3)^-) + 2\,CH_3COO^-)) \quad (1)$$

The Ni-containing material as synthesized by reaction with glycerol, in the presence and absence of KOH (Ni-Gly-KOH and Ni-Gly), were also characterized by FTIR (Fig. S4a) and compared with glycerol and n-butanol. All spectra were very similar but a low intensity band at 1558 cm^{-1} (Fig. S4b), which can be attributed to asymmetric O-C-O stretching vibration modes of carboxylates ions of the Ni-acetate used as reagent, was significantly intensified in Ni-Gly-KOH, but did not provide any additional information. However, the FTIR spectra after thermal treatment at 180 (Ni-Gly-KOH-180) and 240 °C (Ni-Gly-KOH-240) showed the disappearance of the 2935 and 2876 cm^{-1} bands (Fig. 6a), assigned to symmetric and antisymmetric methylene ($–CH_2$) stretching modes, consistent with the oxidation of glycerol to compounds containing carboxylate groups. This assumption is supported by the intensification of the bands at 1560, 1410 and 1348 cm^{-1} attributed to O-C-O stretching vibrational modes [28], and confirmed by the disappearance of the bands in the 1260 cm^{-1} to 800 cm^{-1} range mainly assigned to C—O stretching modes of primary and secondary alcohols, characteristic of glycerol [20,28] (Fig. 6b). This conclusion is also supported by the decrease of the relative intensity of the band at 3400 cm^{-1} (broad peak) of the Ni-Gly-KOH-180 after thermal treatment for 120 min compared to 30 min (at room temperature the amount of n-butanol is relatively high and makes comparison impossible). In fact, the decrease of the O—H stretching mode of hydroxyl groups, [29,30] upon thermal treatment, indicates dehydration and elimination of water, probably forming C=C bonds.

The surface chemical composition and coordination shell in Ni-Gly-KOH-240 were further analyzed by X-ray photoelectron spectroscopy (XPS). The XPS survey spectrum showed that it is constituted mainly by

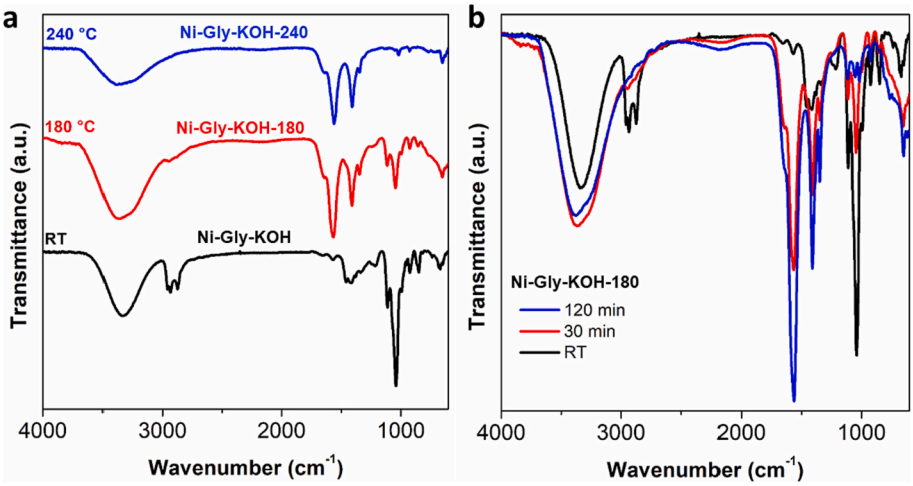

Fig. 6. (a) FTIR spectra of Ni-Gly-KOH before (black line, Ni-Gly-KOH) and after thermal treatment at 180 (red line, Ni-Gly-KOH-180) and 240 °C (blue line, Ni-Gly-KOH-240) for 30 min. (b) Comparison of the FTIR spectra for Ni-Gly-KOH after heat treatment for 30 and 120 min at 180 °C. (For interpretation of the references to colour in this figure legend, the reader is referred to the web version of this article.)

Ni, K, O and C (Fig. 7a), as expected for a sample containing organic material and without a previous washing process. The high-resolution XPS Ni 2p deconvoluted spectra for Ni-Gly-KOH-240, shown in Fig. 7c, is in good agreement with the reference spectrum of a standard Ni^{2+} sample. In fact, only two spin-orbit doublets can be observed, assigned to Ni $2p_{3/2}$ and Ni $2p_{1/2}$ at 855.3 eV and 872.8 eV, and the corresponding shake-up satellites close to the peaks which can be attributed to the presence of Ni^{2+} coordinated to O-donors in the material [31]. In addition, the spin-orbital coupling energy separation of 17.5 eV of Ni $2p_{3/2}$ and Ni $2p_{1/2}$ is characteristic of Ni^{2+} [32,33]. Also, it is important to mention that the presence of a shoulder at 854.26 eV may be associated with the formation of NiO [20] thus supporting our assumption. On the other hand, it is also clearly visible an another shoulder at 881.3 eV, typically assigned to the presence of some oxidized Ni^{3+} cation. The high-resolution C1s spectrum of the Ni-Gly-KOH-240 film shows four main peaks at 284.1, 284.6, 285.3, and 287.9 eV, corresponding to the C═C, C—C, C—O, and C═O (Fig. 7b), which implies that some oxidized organic molecules with C/O functional groups, such as acetate, are present after the thermal treatment. Furthermore, the significant presence of C═O and C═C bonds is consistent with the FTIR results. Finally, the high-resolution O1s spectrum were deconvoluted into four components at 530.2, 530.7, 531.4, and 532.4 eV which were assigned to oxygen forming Ni—O, C—O, C-OH and C═O bonds (Fig. 7d).

The presence of organic compounds even after thermal treatment is also confirmed by cyclic voltammetry (Fig. 8). In fact, in the first voltammetric cycle (Fig. 8a and 8b), an irreversible oxidation process appears at approximately 0.45 V *vs.* Ag/AgCl, as expected for the oxidation of organic molecules promoted by electrode materials with Ni^{3+} as electrocatalytic active sites [11]. In addition, the anodic peak (shoulder) at 0.38 V *vs.* Ag/AgCl is attributed to the oxidation of $Ni(OH)_2$ to NiOOH, whereas a low-intensity cathodic peak at 0.27 V *vs.* Ag/AgCl is

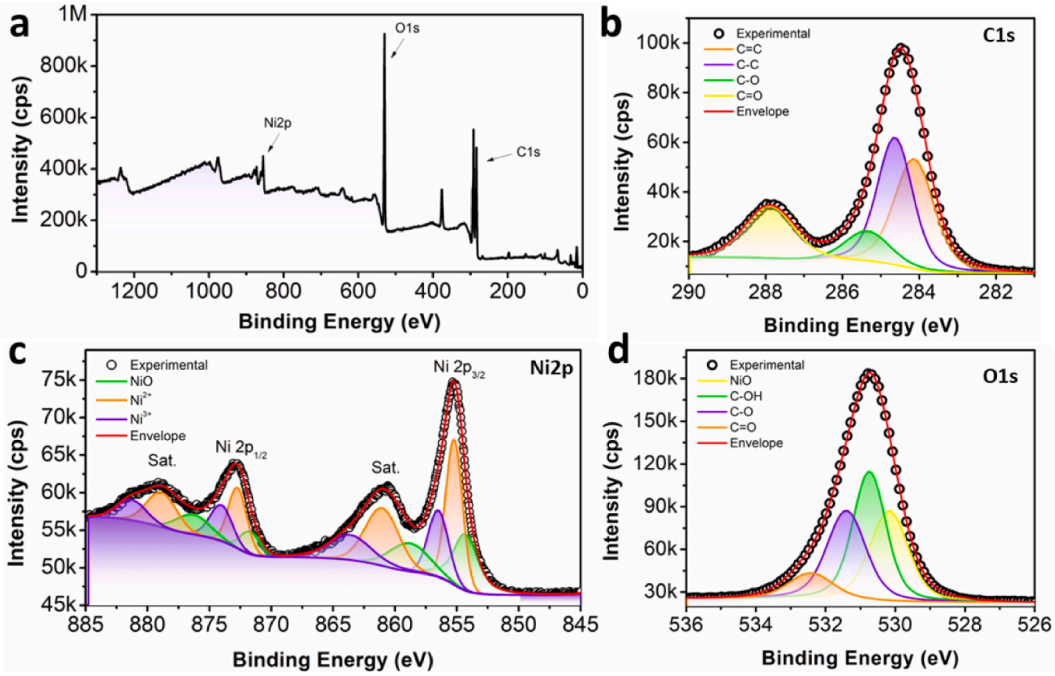

Fig. 7. (a) XPS survey spectrum, and high-resolution XPS spectra for (b) C1s, (c) Ni 2p and (d) O1s for Ni-Gly-KOH-240.

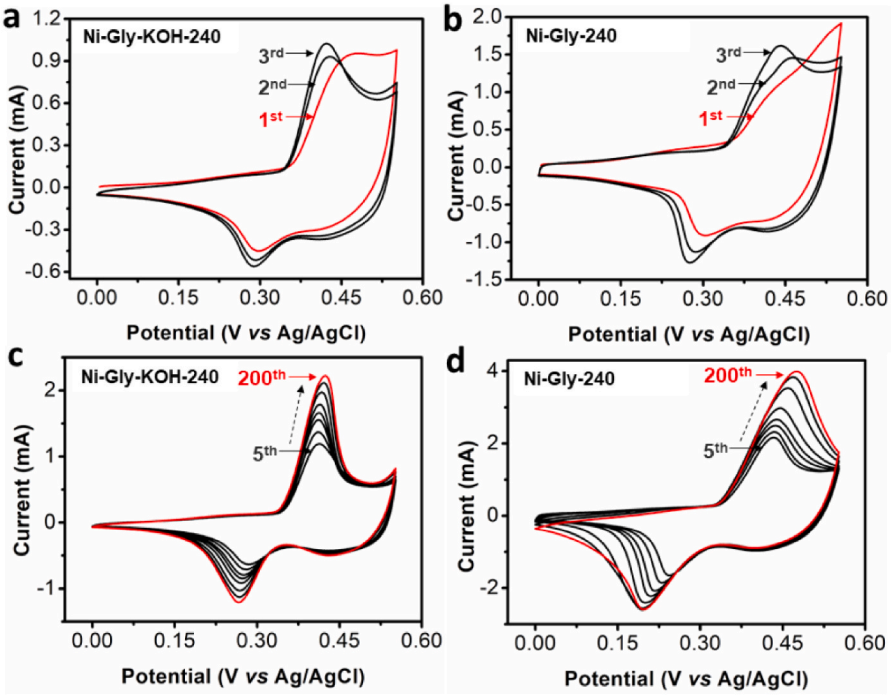

Fig. 8. (a-b) First 3 cyclic voltammograms (1st, 2nd and 3rd) and (c-d) the 5th, 10th, 20th, 30th, 50th, 100th, 150th e 200th following successive cyclic voltammograms of a Ni-Gly-KOH (a and c) and Ni-Gly-240 (b-d) modified FTO electrodes after thermal treatment at 240 °C for 30 min. v = 50 mV s^{-1}, in 1.0 mol L^{-1} KOH solution.

related to the corresponding reverse reaction. The results here show that the redox peaks of $Ni(OH)_2$ and NiOOH do not appear with high intensity in the first scan (the red curves in Fig. 8a and Fig. 8b), indicating a low amount of $Ni(OH)_2$/NiOOH-based sites. Note that both electrode materials present an increase of the current as a function of the number of CV cycles (Fig. 8c and 8d). This behavior is attributed to the progressive diffusion of the electrolyte solution into the film, generating more and more Ni-hydroxide redox active sites. Furthermore, it is important to mention that the *in-situ* formation of new Ni-hydroxide sites occurs under alkaline conditions concomitantly with the oxidation of organic molecules present in both electrode materials. In general, metal−glycerolate based materials tend to be converted to the corresponding metal oxyhydroxide or metal hydroxide based materials exhibiting excellent electrocatalytic activity under alkaline conditions [12]. This is a well-reported strategy used to prepare electrocatalysts for oxygen evolution reaction (OER) and hybrid supercapacitors based on metal-glycerolates, oxides and sulfides [34].

Finally, it is important to mention that Rocha et al. [2] reported the formation of α-$Ni(OH)_2$ nanoparticles based on the analysis of the solid material by transmission electron microscopy which may have been formed *in-situ* by the electron beam during the measurement. However, many works in the literature show that there is formation of metal-glycerolate [25] or metal-glycerol complex [35] in similar reaction systems involving metal ions and glycerol in the presence or absence of KOH. Furthermore, the hydrolysis reaction of metal glycerolates generally results in the formation of the thermodynamically stable β-$Ni(OH)_2$ phase [16,17], in contrast to the α-$Ni(OH)_2$ reported by Rocha et al. [2].

In order to shed light on this dilemma, it is important to examine the pK_a's of glycerol, n-butanol, water and acetic acid whose acid-base reactions are more or less contributing to the material formed in the Tower's and other similar reactions. When a nickel salt is dissolved in glycerol, the most probable reaction is a relatively strong electrostatic interaction of Ni^{2+} ions with the counter ion and coordination/solvation by glycerol. The incorporation of alcohols such as isopropanol should decrease their solubility leading to formation of particles, as described by Wang et al. [36] that autoclaved 7.5 mL of glycerol, 0.145 g of $Ni(NO_3)_2.6H_2O$ and 52.5 mL of isopropanol at 180 °C for 12 h, to get solid Ni-glycerate (should be called Ni-glycerolate) after cooling naturally until the room temperature. Isopropanol is similar to n-butanol (pKa 16.1) and is much less acidic than glycerol (pKa 14.4) and nitric acid, a strong mineral acid. Thus, nitrate ion, neither the hydration water molecules, does not have enough basicity to deprotonate glycerol and generate glycerolates, but isopropanol can induce the formation of nickel acetate precipitate. Considering the obtained solid and a characteristic XRD peak at ~10°, probably the high temperature was enough to dissolve it all and the slow precipitation led to formation of a layered material.

Considering the Tower's method, the reaction of KOH in alcohol solution with nickel acetate dissolved in glycerol results in the formation of a gel, whereas a sol is always formed upon reaction with 2 equivalent of KOH or less [2]. Clearly acetate (acetic acid pKa 4.8) cannot deprotonate glycerol (pKa = 14.4) to glycerolate such that acetate ligands must be coordinated to the Ni^{2+} ions while their remaining coordination sites are occupied by glycerol molecules. However, KOH (pKa ~ 14) is a strong enough base to generate glycerolate in solution, but the relative amount of hydroxide is not enough to convert it in large extent, such that both ought to be coordinated to the Ni^{2+} sites, as well as neutral glycerol molecules to complete the coordination sphere. In addition, it is known that metal oxides [15,37,38] and metal hydroxides [37–39] can react with glycerol to form metal-glycerolates upon thermal treatment, depending on their basicity and the concomitant removal of water molecules formed in the reaction to shift the reaction to the right.

Finally, the reducing properties of organic molecules at high temperatures is well established, as well as the capability of hydroxide/oxide ligands in stabilizing metal ions, such that the formation of Ni metal or NiO upon heat treatment will depend on the relative amounts of Ni^{2+}, hydroxide and organic molecules, mainly as glycerolate/glycerol (and acetate) present in the material. But, considering the 1:2 proportion of Ni^{2+}/OH^- utilized in the reaction, the formation of $Ni(OH)_2$ seems to

be rather improbable, corroborating our hypothesis that $Ni(OH)_2$ is only formed when the Ni^{2+}-hydroxide/glycerolate/acetate is put in contact and react with an aqueous alkaline solution, due to the hydrolysis of the material prepared by Tower's method.

4. Conclusion

Tower's method has been extensively used in the development of electroactive materials for several electrochemical applications. However, based on XRD data, the materials resulting from the Tower's method show strikingly similar structures to metal-glycerolates prepared by solvothermal methods using similar reagents. In this sense, Ni-based materials were carefully prepared and analyzed by structural, morphological, spectroscopic, and electrochemical characterization techniques. However, HRTEM images and UV–vis measurements showed no evidence of nanoparticles. In addition, a lamellar structure is only formed in the material incorporating KOH indicating its key role in the glycerol deprotonation reaction. Furthermore, a systematic study by FTIR spectroscopy brought compelling evidence on the possible dehydration reaction of glycerol induced by thermal treatment, and of the nickel-complex derivatives, promoting the formation of metal glycerolates with more or less organized lamellar structure, as evidenced by the sharp XRD peak at 10.5°. Summarizing, Ni-glycerolate is the most probable product of Tower's method after thermal processing, as a consequence of the reaction of glycerol with OH^- followed by elimination of water during the thermal treatment up to 240 °C. However, metallic nickel nanoparticles are obtained at higher calcination temperatures, and/or irradiation with electron beam during electron microscopy assays, indicating that nickel hydroxide nanoparticles are only formed upon further reaction with an aqueous alkaline solution. In short, Ni-Gly materials obtained by Tower's method are interesting as precursors for the design and preparation of new electrode nanomaterials for energy conversion and storage such as supercapacitors, as well as electrocatalysts and electrochemical sensors.

Supplementary data to this article can be found online at https://doi.org/10.1016/j.matchar.2022.112636.

Declaration of Competing Interest

The authors declare that they have no known competing financial interests or personal relationships that could have appeared to influence the work reported in this paper.

Data availability

The Data that support the findings of this study are available from the corresponding author upon reasonable request.

Acknowledgments

This work was partially supported by the Sao Paulo Research Foundation (FAPESP processes 2018/16896-7, 2018/21489-1 and 2020/06176-7) by the National Council for Scientific and Technological Development (CNPq Processes 307271/2017-0, 304651/2021-4, 442599/2019-6 and 311847/2018-8), INCTBio (CNPq grant no. 465389/2014–7), and INCT/FAPESP (Process 2014/50867-3). R. Shahbazian-Yassar and A. Phakatkar are thankful to financial support from U.S. National Science Foundation (NSF) award DMR-1809439. The authors also thank SisNANO-USP for the use of FTIR/XRD facility. Electron microscopy experiments were supported by NSF award CDS&E-2055442.

References

[1] O.F. Tower, Note on colloidal nickel hydroxide, J. Phys. Chem. 28 (1924) 176–178, https://doi.org/10.1021/j150236a009.

[2] M.A. Rocha, H. Winnischofer, K. Araki, F.J. Anaissi, H.E. Toma, A new insight on the preparation of stabilized alpha-nickel hydroxide nanoparticles, J. Nanosci. Nanotechnol. 11 (2011) 3985–3996, https://doi.org/10.1166/jnn.2011.3872.

[3] J.M. Gonçalves, T.A. Matias, L.P.H. Saravia, M. Nakamura, J.S. Bernardes, M. Bertotti, K. Araki, Synergic effects enhance the catalytic properties of alpha-Ni$(OH)_2$-FeOCPc@rGO composite for oxygen evolution reaction, Electrochim. Acta 267 (2018) 161–169. http://www.sciencedirect.com/science/article/pii/S0013468618303712.

[4] P.O. Rossini, A. Laza, N.F.B. Azeredo, J.M. Gonçalves, F.S. Felix, K. Araki, L. Angnes, Ni-based double hydroxides as electrocatalysts in chemical sensors: a review, TrAC Trends Anal. Chem. 126 (2020), 115859, http://www.sciencedirect.com/science/article/pii/S0165993620300881.

[5] R.J. Mortimer, M.Z. Sialvi, T.S. Varley, G.D. Wilcox, An in situ colorimetric measurement study of electrochromism in the thin-film nickel hydroxide/oxyhydroxide system, J. Solid State Electrochem. 18 (2014) 3359–3367, https://doi.org/10.1007/s10008-014-2618-5.

[6] K. Liu, W. Zhou, D. Zhu, J. He, J. Li, Z. Tang, L. Huang, B. He, Y. Chen, Excellent high-rate capability of micron-sized co-free α-$Ni(OH)_2$ for high-power Ni-MH battery, J. Alloys Compd. 768 (2018) 269–276. http://www.sciencedirect.com/science/article/pii/S0925838818326598.

[7] J.M. Gonçalves, K.M. Alves, M.F. Gonzalez-Huila, A. Duarte, P.R. Martins, K. Araki, Unexpected stabilization of α-$Ni(OH)_2$ nanoparticles in GO nanocomposites, J. Nanomater. 2018 (2018) 5735609, https://doi.org/10.1155/2018/5735609.

[8] K.W. Kwan, S.J. Li, N.Y. Hau, W.-D. Li, S.P. Feng, A.H.W. Ngan, Light-stimulated actuators based on nickel hydroxide-oxyhydroxide, Sci. Robot. 3 (2018) eaat4051, https://doi.org/10.1126/scirobotics.aat4051.

[9] A.P. Gomes, J.M. Gonçalves, K. Araki, P.R. Martins, Enhancement of stability and specific charge capacity of alpha-$Ni(OH)_2$ by Mn(II) isomorphic substitution, Energy Technol.-Ger. 7 (2019) 1800980, https://doi.org/10.1002/ente.201800980.

[10] N.F.B. Azeredo, J.M. Gonçalves, I.S. Lima, K. Araki, J. Wang, L. Angnes, Screen-printed nickel-cerium Hydroxide sensor for acetaminophen determination in body fluids, Chemelectrochem 8 (2021) 2505–2511, https://doi.org/10.1002/celc.202100417.

[11] G.L.D. Assis, J.M. Gonçalves, J.S. Bernardes, K. Araki, Nickel-cerium layered double hydroxide as electrocatalyst for glycerol oxidation, J. Braz. Chem. Soc. 31 (2020) 2351–2359, https://doi.org/10.21577/0103-5053.20200131.

[12] J.M. Gonçalves, A.L. Hennemann, J.G. Ruiz-Montoya, P.R. Martins, K. Araki, L. Angnes, R. Shahbazian-Yassar, Metal-glycerolates and their derivatives as electrode materials: a review on recent developments, challenges, and future perspectives, Coord. Chem. Rev. 477 (2023) 214954. https://www.sciencedirect.com/science/article/pii/S0010854522005495.

[13] S. Ding, J. An, D. Ding, Y. Zou, L. Zhao, Micron-sized NiMn-glycerate solid spheres as cathode materials for all-solid-state asymmetric supercapacitor with superior energy density and cycling life, Chem. Eng. J. 431 (2022), 134100, https://www.sciencedirect.com/science/article/pii/S1385894721056746.

[14] M. Wang, J. Jiang, L. Ai, Layered bimetallic iron–nickel alkoxide microspheres as high-performance electrocatalysts for oxygen evolution reaction in alkaline media, ACS Sustain. Chem. Eng. 6 (2018) 6117–6125, https://doi.org/10.1021/acssuschemeng.7b04784.

[15] T.Y.G. Khonina, E.Y. Nikitina, A.Y. Germov, B.Y. Goloborodsky, K.N. Mikhalev, E. A. Bogdanova, D.S. Tishin, A.M. Demin, V.P. Krasnov, O.N. Chupakhin, V. N. Charushin, Individual iron(III) glycerolate: synthesis and characterisation, RSC Adv. 12 (2022) 4042–4046, https://doi.org/10.1039/D1RA08485B.

[16] C. Cheng, C. Wei, Y. He, L. Liu, J. Hu, W. Du, Etching strategy synthesis of hierarchical Ni-Mn hydroxide hollow spheres for supercapacitors, J. Energy Storage 33 (2021), 102105, https://www.sciencedirect.com/science/article/pii/S2352152X20319356.

[17] J. Zhao, Y. Zou, X. Zou, T. Bai, Y. Liu, R. Gao, D. Wang, G.-D. Li, Self-template construction of hollow Co_3O_4 microspheres from porous ultrathin nanosheets and efficient noble metal-free water oxidation catalysts, Nanoscale 6 (2014) 7255–7262, https://doi.org/10.1039/C4NR00002A.

[18] J.M. Gonçalves, I.S. Lima, N.F.B. Azeredo, D.P. Rocha, A. de Siervo, L. Angnes, NiVCe-layered double hydroxide as multifunctional nanomaterials for energy and sensor applications, Front. Mater. 8 (2021), https://doi.org/10.3389/fmats.2021.781900.

[19] A.L. Correa, J.M. Gonçalves, P.O. Rossini, J.S. Bernardes, C.A. Neves, K. Araki, L. Angnes, Fast and reliable BIA/amperometric quantification of acetylcysteine using a nanostructured double hydroxide sensor, Talanta 186 (2018) 354–361. http://www.sciencedirect.com/science/article/pii/S0039914018304090.

[20] J.M. Gonçalves, R.R. Guimarães, B.B.N.S. Brandão, L.P.H. Saravia, P.O. Rossini, C. V. Nunes, J.S. Bernardes, M. Berttoti, L. Angnes, K. Araki, Nanostructured alpha-NiCe mixed hydroxide for highly sensitive amperometric prednisone sensors, Electrochim. Acta 247 (2017) 30–40. http://www.sciencedirect.com/science/article/pii/S0013468617314044.

[21] N.F.B. Azeredo, J.M. Gonçalves, P.O. Rossini, K. Araki, J. Wang, L. Angnes, Uric acid electrochemical sensing in biofluids based on Ni/Zn hydroxide nanocatalyst, Microchim. Acta 187 (2020) 379, https://doi.org/10.1007/s00604-020-04351-2.

[22] M. Kim, W.-S. Son, K.H. Ahn, D.S. Kim, H.-S. Lee, Y.-W. Lee, Hydrothermal synthesis of metal nanoparticles using glycerol as a reducing agent, J. Supercrit. Fluids 90 (2014) 53–59. https://www.sciencedirect.com/science/article/pii/S0896844614000618.

[23] K. Singh, K.H. Kate, V.V.S. Chilukuri, P.K. Khanna, Glycerol mediated low temperature synthesis of nickel nanoparticles by solution reduction method, J. Nanosci. Nanotechnol. 11 (2011) 5131–5136.

[24] M. Tanaka, M. Takeguchi, K. Furuya, Behavior of metal nanoparticles in the electron beam, Micron 33 (2002) 441–446. https://www.sciencedirect.com/science/article/pii/S0968432801000464.
[25] J. Teichert, T. Block, R. Pöttgen, T. Doert, M. Ruck, Tin and lead alkoxides of ethylene glycol and glycerol and their decomposition to oxide materials, Eur. J. Inorg. Chem. 2019 (2019) 3820–3831, https://doi.org/10.1002/ejic.201900755.
[26] M.A. Rocha, F.J. Anaissi, H.E. Toma, K. Araki, H. Winnischofer, Preparation and characterization of colloidal $Ni(OH)_2$/bentonite composites, Mater. Res. Bull. 44 (2009) 970–976. http://www.sciencedirect.com/science/article/pii/S002554080800411X.
[27] I. Pelivanov, E. Petrova, S.J. Yoon, Z. Qian, K. Guye, M. O'Donnell, Molecular fingerprinting of nanoparticles in complex media with non-contact photoacoustics: beyond the light scattering limit, Sci. Rep.-Uk 8 (2018) 14425, https://doi.org/10.1038/s41598-018-32580-2.
[28] J.F. Gomes, A.C. Garcia, L.H.S. Gasparotto, N.E. de Souza, E.B. Ferreira, C. Pires, G. Tremiliosi-Filho, Influence of silver on the glycerol electro-oxidation over AuAg/C catalysts in alkaline medium: a cyclic voltammetry and in situ FTIR spectroscopy study, Electrochim. Acta 144 (2014) 361–368. https://www.sciencedirect.com/science/article/pii/S0013468614016582.
[29] T.G. Ritter, A.H. Phakatkar, M.G. Rasul, M.T. Saray, L.V. Sorokina, T. Shokuhfar, J. M. Gonçalves, R. Shahbazian-Yassar, Electrochemical synthesis of high entropy hydroxides and oxides boosted by hydrogen evolution reaction, Cell Rep. Phys. Sci. 3 (2022) 100847. https://www.sciencedirect.com/science/article/pii/S2666386422001217.
[30] S.M. Yakout, Remarkable magnetic properties of undoped NiO-based nanocomposites: size and surface/interface effects, J. Mater. Sci. Mater. Electron. 28 (2017) 14348–14361, https://doi.org/10.1007/s10854-017-7295-6.
[31] B.N. Safadi, J.M. Gonçalves, E. Castaldelli, T.A. Matias, P.O. Rossini, M. Nakamura, L. Angnes, K. Araki, Lamellar FeOcPc-Ni/GO composite-based enzymeless glucose sensor, Chemelectrochem 7 (2020) 2553–2563, https://doi.org/10.1002/celc.202000138.
[32] Z. Liu, H. Zhou, F. Zeng, L. Hu, X. Wu, X. Song, C. Jiang, X. Zhang, All-printed high-performance flexible supercapacitors using hierarchical porous nickel–cobalt hydroxide inks, ACS Appl. Energy Mater. (2022), https://doi.org/10.1021/acsaem.2c00947.
[33] J. Yang, C. Yu, C. Hu, M. Wang, S. Li, H. Huang, K. Bustillo, X. Han, C. Zhao, W. Guo, Z. Zeng, H. Zheng, J. Qiu, Surface-confined fabrication of ultrathin nickel cobalt-layered double hydroxide nanosheets for high-performance supercapacitors, Adv. Funct. Mater. 28 (2018) 1803272, https://doi.org/10.1002/adfm.201803272.
[34] M.I. da Silva, Í.R. Machado, H.E. Toma, K. Araki, L. Angnes, J.M. Gonçalves, Recent progress in water-splitting and supercapacitor electrode materials based on MOF-derived sulfides, J. Mater. Chem. A 10 (2022) 430–474, https://doi.org/10.1039/D1TA05927K.
[35] Y. Li, M. Cai, J. Rogers, Y. Xu, W. Shen, Glycerol-mediated synthesis of Ni and Ni/NiO core-shell nanoparticles, Mater. Lett. 60 (2006) 750–753, https://www.sciencedirect.com/science/article/pii/S0167577X05009699.
[36] J. Wang, B. Wang, X. Liu, G. Wang, H. Wang, J. Bai, Construction of carbon-coated nickel phosphide nanoparticle assembled submicrospheres with enhanced electrochemical properties for lithium/sodium-ion batteries, J. Colloid Interface Sci. 538 (2019) 187–198. https://www.sciencedirect.com/science/article/pii/S0021979718314152.
[37] I. Reyero, G. Arzamendi, L.M. Gandía, Heterogenization of the biodiesel synthesis catalysis: CaO and novel calcium compounds as transesterification catalysts, Chem. Eng. Res. Des. 92 (2014) 1519–1530. https://www.sciencedirect.com/science/article/pii/S026387621300508X.
[38] N. Ebadi Pour, F. Dumeignil, B. Katryniok, L. Delevoye, B. Revel, S. Paul, Investigating the active phase of Ca-based glycerol polymerization catalysts: on the importance of calcium glycerolate, Mol. Catal. 507 (2021) 111571. https://www.sciencedirect.com/science/article/pii/S2468823121001887.
[39] H. Cheng, J. Wei, M. Liang, S. Dai, X. Liu, L. Ma, H. Wang, F. Lai, Calcium glycerolate catalyst derived from eggshell waste for cyclopentadecanolide synthesis, Front. Chem. 9 (2021), https://doi.org/10.3389/fchem.2021.770247.